Design for electromagnetic wave transparency with metamaterials

Xiaoming Zhou and Gengkai Hu*
School of Science, Beijing Institute of Technology, Beijing 100081, People's Republic of China
(Received 18 May 2006; published 21 August 2006)

With the help of the "neutral inclusion" concept, the conditions of electromagnetic wave transparency for multilayered spheres, coated spheroids, and general particulate composites are analytically derived in the quasistatic case. The basic idea is to make the effective material property of a composite region equal to that of the surrounding medium. The general *full-wave* analysis shows that the obtained quasistatic conditions are useful in designing the electromagnetically transparent materials.

DOI: 10.1103/PhysRevE.74.026607 PACS number(s): 42.70.−a, 42.79.−e, 42.50.Gy, 33.20.Fb

I. INTRODUCTION

There are basically two ways to achieve "low observability" for an object in electromagnetic waves. One is based on an absorption mechanism, such as the use of absorbing screens [1] and radar absorbing materials [2]. The other way is to make an object "transparent" to the wave. The transparency can be realized by many mechanisms; for example, antireflection coatings [3] have been commonly used. Recently, the transparency has been obtained based on new mechanisms [9–12] brought by metamaterials. Metamaterials are artificially fabricated materials. They can be designed to have unusual properties not found in conventional materials. The left-handed material [4], one type of metamaterial, has negative permittivity and negative permeability, which are realized through electrically and magnetically resonant structures [5,6], respectively. Experiments have shown that this material can exhibit negative refraction [7,8].

Multilayered structures with metemeterial can be transparent to the electromagnetic (EM) wave based on the unusual photon tunneling effect [9,10]. Two-dimensional plasmonic metamaterial can also be transparent for an EM wave if its impedance matches perfectly to vacuum [11]. These two methods are suitable for planar or nearly planar transparent objects. Recently, a more striking method has been proposed by Alù and Engheta [12]. They utilized a plasmonic or metamaterial coating to cover a spherical or cylindrical dielectric core. By adjusting the material and geometrical parameters, they found that at certain configuration, the total scattering cross section of this coated sphere can be extremely low. That work introduced a new way to achieve the "invisibility." In this paper, we continue to discuss this method and emphasize primarily how to achieve transparency for other objects, such as multilayered spheres, coated spheroids, and two-phase composites. To this end, we will propose an idea based on "neutral inclusion" to derive the transparency condition in the quasistatic case. The obtained condition will be further checked by a full-wave analysis.

II. THEORETICAL ANALYSIS

As shown in Fig. 1, consider a random-shaped region with permittivity ε_* and permeability μ_* embedded in an infinite matrix of permittivity ε_m and permeability μ_m; a plane wave propagates through this medium. The region can be made of either a homogeneous medium or a heterogeneous material. For the latter, ε_* and μ_* then denote the effective permittivity and effective permeability of the heterogeneous material. It is not surprising that if the material property of this region is the same as that of the background medium (matrix), the electromagnetic field outside of this region will not be disturbed. In other words, the region will not be "seen" by the outside observer. The basic idea of this paper is to derive the condition for electromagnetic wave transparency. When the region is made of a homogeneous material, this is a trivial case. However, if the region is made of a heterogeneous material, there are many design possibilities for equating its effective material property to that of the background medium. In order to proceed, we will recall the concept of "neutral inclusion" discussed extensively by Milton [13]. A neutral inclusion is a simple pattern (coated sphere, coated spheroid, etc.). When a neutral inclusion is embedded in a material made of assemblages of such a pattern with gradual size (in order to fill the whole space), it will not perturb the static electric, magnetic, or mechanical fields outside of this inclusion. Although the neutral inclusion is defined in the static or quasistatic case, it can still provide useful information in the full-wave scattering case.

We first apply this idea to the coated sphere that has been analyzed by Alù and Engheta [12]. Suppose that a sphere of radius r_1 is covered with a coating of radius r_2. The relative permittivities of the nonmagnetic core and coating are denoted by ε_1 and ε_2, respectively. In order to make this coated sphere a neutral inclusion with respect to the surrounding air, the effective permittivity ε_* of an assemblage of coated

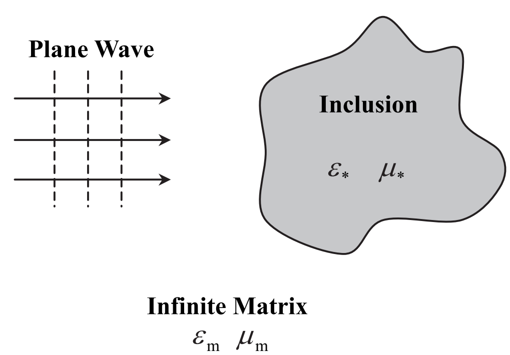

FIG. 1. Example of neutral inclusion.

*Author to whom all correspondence should be addressed. Email address: hugeng@bit.edu.cn

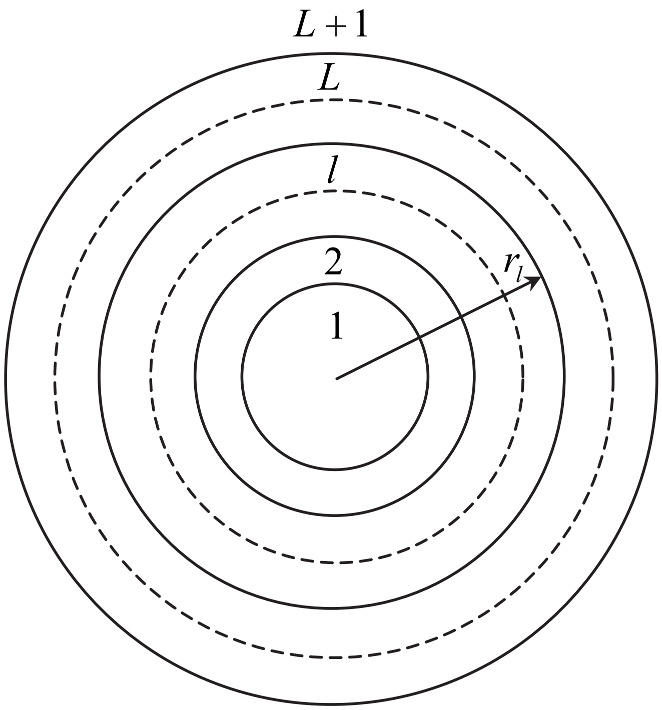

FIG. 2. Cross section of a multilayered sphere.

spheres with the gradual size needs to be equal to that of the air, i.e., we need to set $\varepsilon_* = 1$. In the quasistatic case, the effective permittivity ε_* of the coated sphere assemblage can be estimated simply from the Maxwell-Garnett formula [14],

$$\varepsilon_* = \varepsilon_2 + \frac{3f_1\varepsilon_2(\varepsilon_1 - \varepsilon_2)}{3\varepsilon_2 + f_2(\varepsilon_1 - \varepsilon_2)}, \tag{1}$$

where $f_1 = 1 - f_2 = r_1^3/r_2^3$ is the volume fraction of the core particle. For the "invisibility," the general condition $\varepsilon_* = 1$ leads to the following relation:

$$\frac{(\varepsilon_2 - 1)(2\varepsilon_2 + \varepsilon_1)}{(2\varepsilon_2 + 1)(\varepsilon_2 - \varepsilon_1)} = \frac{r_1^3}{r_2^3}. \tag{2}$$

Equation (2) is exactly the same as that derived by Alù and Engheta [12]. Actually, the effective permittivity given by Eq. (1) provides the bound for any isotropic two-phase composite [15]. This indicates that the effective permittivity can never be lower than unity if each phase of the composite is a conventional material. However, by introducing metamaterial whose permittivity and/or permeability are often less than unity, many new features may arise. For example, we can design a composite with unit effective permittivity and effective permeability if metamaterials are introduced.

Encouraged by the above result, the quasistatic transparency conditions will be derived for several other structures in the following. Without loss of generality, these conditions will be given for nonmagnetic materials.

A. Multilayered sphere

Now we apply the idea of "neutral inclusion" to a multilayered sphere whose cross section is shown in Fig. 2. Each region ($l = 1, 2, \ldots, L$) is characterized by relative permittivity ε_l, relative permeability μ_l, refractive index $m_l = n_l / n_{L+1}$ ($n_l = \sqrt{\varepsilon_l}\sqrt{\mu_l}$), and size parameter $x_l = 2\pi r_l / \lambda_0$, where λ_0 is the free-space wavelength and r_l is the outer radius of the lth layer. In Mie theory, the scattering coefficients a_n and b_n can be calculated, which are given in the Appendix. The full-wave total scattering cross section of this multilayered sphere Q_s can be computed by

$$Q_s = \frac{\lambda_0^2}{2\pi}\sum_{n=1}^{\infty}(2n+1)(|a_n|^2 + |b_n|^2). \tag{3}$$

In order to make this multilayered sphere "invisible," we have to reduce the total cross section Q_s. A direct way of accomplishing this is to make zero the scattering coefficients a_n and b_n. When the scatterer is small enough compared with the wavelength of operation [Rayleigh approximation (RA)], we need only consider the influence of the first-order [$n=1$ in Eq. (3)] scattering coefficients. The conditions of validity of this approximation are $\{\max(|m_l x_l|, |m_{l+1} x_l|), l = 1, 2, \ldots, L\} \ll 1$. Low observable conditions can then be derived, following the same process for a coated sphere [12].

Here, we will use the concept of "neutral inclusion" to derive the transparency condition in a simple and direct way. To do this, first we compute the effective permittivity of the assemblage of multilayered spheres. This can be evaluated through a recursive method by considering the l-layer sphere as an effective core embedded in the lth-coating material. The effective permittivity ε_*^l of the l-layer sphere assemblage is then calculated by [13]

$$\varepsilon_*^l = \varepsilon_l + \frac{3(1 - f_l)\varepsilon_l(\varepsilon_*^{l-1} - \varepsilon_l)}{3\varepsilon_l + f_l(\varepsilon_*^{l-1} - \varepsilon_l)}, \quad l = 3, 4, \ldots, L, \tag{4}$$

where $f_l = 1 - r_{l-1}^3 / r_l^3$ is the volume fraction of the lth layer in the l-layer sphere. ε_*^2 (the effective permittivity of the coated sphere assemblage) is calculated from Eq. (1). The transparency condition for the multilayered sphere can then be obtained by setting $\varepsilon_*^L = 1$. For a doubly coated sphere, the transparency condition becomes

$$\frac{r_2^3(2\varepsilon_3 + 1)}{r_3^3(\varepsilon_3 - 1)} = \frac{2(r_2^3 - r_1^3)(\varepsilon_1\varepsilon_3 + \varepsilon_2^2) + 2(2r_2^3 + r_1^3)\varepsilon_2\varepsilon_3 + (r_2^3 + 2r_1^3)\varepsilon_1\varepsilon_2}{(r_2^3 - r_1^3)(\varepsilon_1\varepsilon_3 - 2\varepsilon_2^2) + (2r_2^3 + r_1^3)\varepsilon_2\varepsilon_3 - (r_2^3 + 2r_1^3)\varepsilon_1\varepsilon_2}. \tag{5}$$

If material and geometrical parameters of a doubly coated sphere satisfy Eq. (5), in the RA this composite sphere will not perturb the EM wave when it is placed in the air.

B. Coated spheroid

Following the "neutral inclusion" concept, we can easily derive the transparency condition for a nonspherical particle system, for example the double-layer confocal spheroid. In the Cartesian coordinates (x, y, z), the semiaxes of the core and mantle are denoted by a_l, a_l, and ρa_l ($l=1$ for the core, $l=2$ for the mantle), respectively, where ρ is the aspect ratio of the spheroid. Due to the shape asymmetry, the overall property of the assemblage of aligned double-layer confocal spheroids will be anisotropic if the core and mantle are all isotropic. So we introduce an anisotropic core to cancel the shape anisotropy and to make this double-layer spheroid effectively isotropic. In the coordinate system mentioned above, an anisotropic core of permittivity tensor $\tilde{\varepsilon}_1 = (\varepsilon_1, \varepsilon_1, \eta\varepsilon_1)$, which has only three diagonal components, is used and covered with an isotropic coating of permittivity ε_2. The effective permittivity tensor of the composite filled with such a coated spheroid is then given by $\tilde{\varepsilon}_* = (\varepsilon_{11}^*, \varepsilon_{22}^*, \varepsilon_{33}^*)$, where [16]

$$\varepsilon_{11}^* = \varepsilon_{22}^* = \varepsilon_2 + \frac{f(\varepsilon_1 - \varepsilon_2)\varepsilon_2}{\varepsilon_2 + P(1-f)(\varepsilon_1 - \varepsilon_2)}, \tag{6}$$

$$\varepsilon_{33}^* = \varepsilon_2 + \frac{f(\eta\varepsilon_1 - \varepsilon_2)\varepsilon_2}{\varepsilon_2 + (1-2P)(1-f)(\eta\varepsilon_1 - \varepsilon_2)}, \tag{7}$$

with $f = (a_1/a_2)^3$. For prolate spheroids,

$$P = \frac{1}{2}\left\{1 + \frac{1}{\rho^2 - 1}\left[1 - \frac{1}{2\sqrt{1 - 1/\rho^2}} \times \ln\left(\frac{1 + \sqrt{1 - 1/\rho^2}}{1 - \sqrt{1 - 1/\rho^2}}\right)\right]\right\}, \quad \rho \geqslant 1,$$

and for oblate spheroids,

$$P = \frac{1}{2}\left\{1 + \frac{1}{\rho^2 - 1}\left[1 - \frac{1}{\sqrt{1/\rho^2 - 1}}\tan^{-1}(\sqrt{1/\rho^2 - 1})\right]\right\},$$

$$\rho \leqslant 1.$$

By setting $\varepsilon_{11}^* = \varepsilon_{33}^* \equiv 1$, the transparency condition of this coated spheroid can then be derived. This leads to

$$f = \frac{(\varepsilon_2 - 1)[P\varepsilon_1 + (1-P)\varepsilon_2]}{(\varepsilon_2 - \varepsilon_1)[P + (1-P)\varepsilon_2]}, \tag{8a}$$

$$f = \frac{(\varepsilon_2 - 1)[(1-2P)\eta\varepsilon_1 + 2P\varepsilon_2]}{(\varepsilon_2 - \eta\varepsilon_1)[(1-2P) + 2P\varepsilon_2]}. \tag{8b}$$

It is easy to check that the condition (1) can be recovered when $\rho = 1$ and $\eta = 1$, noting that $P = 1/3$ for this case.

C. Composite material

In the small-particle approximation, a heterogeneous scatterer can be effectively considered as a homogeneous one. By setting the effective permittivity of the heterogeneous scatterer to be that of the surrounding medium, the scatterer will be "invisible." This transparency effect will not be sensitive to the microstructure of the scatterer, and depends only on its overall property. Consider that the shaded area in Fig. 1 represents a two-phase isotropic composite. To achieve the transparency, we need to determine exactly the effective permittivity of the composite. For simplicity, we consider the composite with dispersion particles. In the long-wavelength limit, the effective permittivity can be approximately evaluated by the Maxwell-Garnett formula [14],

$$\varepsilon_* = \varepsilon_2 + \frac{3c_1\varepsilon_2(\varepsilon_1 - \varepsilon_2)}{3\varepsilon_2 + (1-c_1)(\varepsilon_1 - \varepsilon_2)}, \tag{9}$$

where ε_1 and ε_2 are permittivities of the particle and matrix, respectively, and c_1 is the particle volume fraction. The quasistatic transparency condition for this composite can be obtained by setting $\varepsilon_* = 1$.

III. NUMERICAL RESULTS

In this section, we will show how the structures discussed in Sec. II can be made "invisible" in the general full-wave scattering case.

A. Multilayered sphere

Unusual scattering property of a coated sphere with metamaterial has been fully discussed by Alù and Engheta [12]. Here we will provide some additional results by investigating a doubly coated sphere. When the parameters $\varepsilon_1 = 5$, $\varepsilon_2 = 3$, $\varepsilon_3 = -2$, $\mu_1 = \mu_2 = \mu_3 = 1$, and $r_1 = 0.2r_3$ for a doubly coated sphere are considered, the effective permittivity ε_* of the doubly coated sphere assemblage as a function of ratio r_2/r_3 is shown in Fig. 3(a). With the help of Eq. (3), the normalized total scattering cross sections of this doubly coated sphere and a single homogeneous sphere with the permittivity ε_* and radius r_3 as a function of ratio r_2/r_3 are illustrated in Figs. 3(b) and 3(c) for two particle sizes. When the particle size is very small ($r_3 = \lambda_0/100$), the total scattering cross section of the composite sphere is consistent with that of the effective homogeneous sphere and both are significantly reduced around $\varepsilon_* = 1$ [Fig. 3(a)]. This implies that the condition (5) obtained from the quasistatic analysis provides indeed a valid prediction. As a matter of fact, corresponding to the "point" $\varepsilon_* \approx 1$, the doubly coated sphere is an electrically tiny particle, since its effective refractive index is almost equal to that of the air. When the particle size increases ($r_3 = \lambda_0/10$), a significant reduction of the total scattering cross section still exists, but the corresponding ratio r_2/r_3 has been shifted downwards, compared to the quasistatic prediction (the dashed line).

Now another set of parameters is examined for the doubly coated sphere, which is $\varepsilon_1 = -5$, $\varepsilon_2 = 3, \varepsilon_3 = 10$, $\mu_1 = \mu_2 = \mu_3 = 1$, and $r_2 = 1.1r_1$. The effective permittivity of the assemblage is plotted in Fig. 4(a). When the particle size is very small ($r_1 = \lambda_0/100$), a significant reduction of the total scattering cross section is observed at the ratio r_3/r_2 corresponding to $\varepsilon_* = 1$, as shown in Fig. 4(b). A strong resonance is also observed for both the doubly coated sphere and the effective homogeneous sphere around the ratio $r_3/r_2 = 1.13$. The resonance is due to the vanishing denominators of the first-order ($n=1$) scattering coefficients b_n. This effect is classified as the surface mode of the spherical particle [17]. For a small homogeneous sphere of permittivity ε, the appearance of the surface mode corresponds to the condition $\varepsilon = -(n+1)/n$ for the nonmagnetic case [17,18]. It can be found that the condition of the lowest-order mode for a sufficiently small plasmonic sphere is $\varepsilon = -2$. In the small-particle approximation, we may expect that the condition of the lowest-order surface

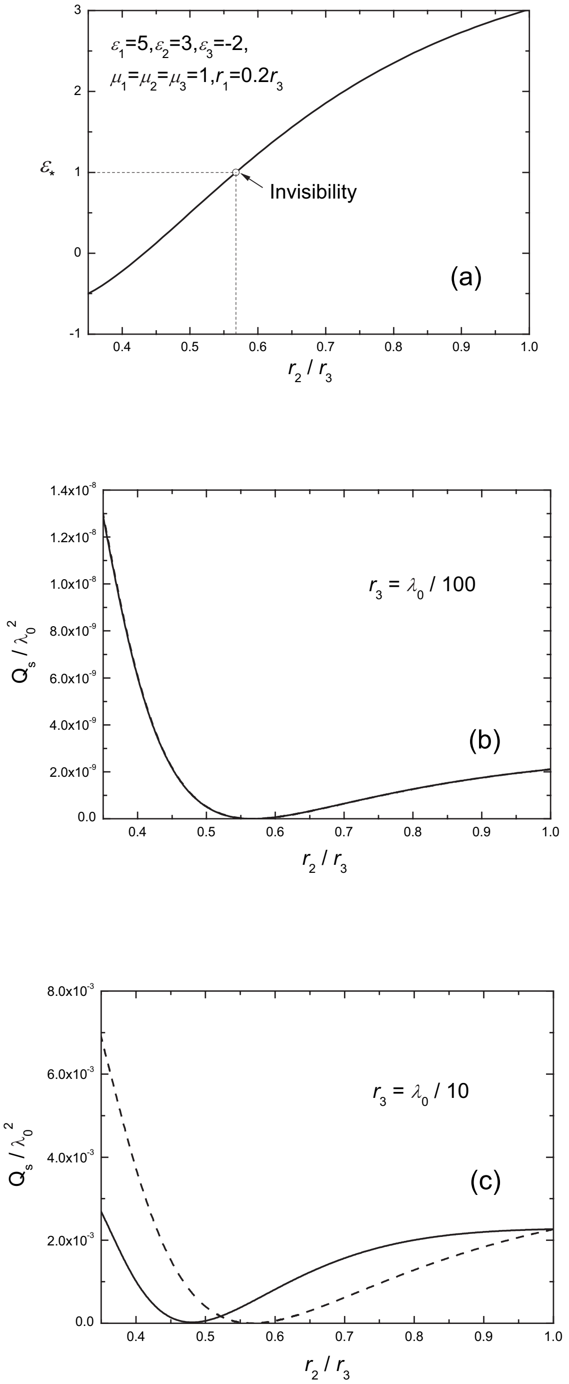

FIG. 3. (a) The effective permittivity ε_* of a doubly coated sphere assemblage calculated from Eq. (4), and (b,c) normalized scattering cross section of a doubly coated sphere (the solid line) and effective homogeneous sphere (the dashed line) with the permittivity ε_* and radius r_3, vs the ratio r_2/r_3 for different r_3.

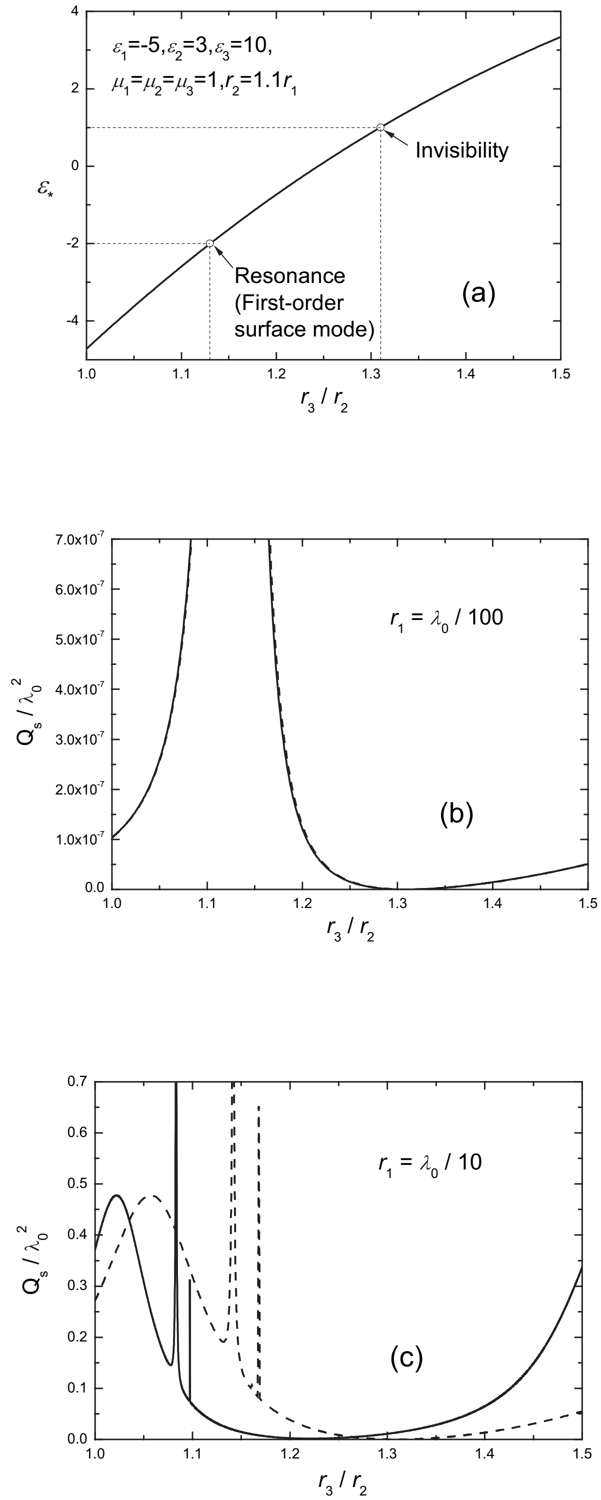

FIG. 4. (a) The effective permittivity ε_* of a doubly coated sphere assemblage calculated from Eq. (4) and (b,c) normalized scattering cross section of a doubly coated sphere (the solid line) and effective homogeneous sphere (the dashed line) with the permittivity ε_* and radius r_3, vs the ratio r_3/r_2 for different r_1.

mode for the multilayered sphere can be given by $\varepsilon_*=-2$, where the effective permittivity ε_* is evaluated analytically from Eq. (4). From Figs. 4(a) and 4(b), it is found that the ratio $r_3/r_2=1.13$ at which the resonance occurs indeed corresponds to $\varepsilon_*=-2$. For a large particle ($r_1=\lambda_0/10$), the second-order ($n=2$) surface mode is also excited. This can be seen from the dashed curve in Fig. 4(c), where the lower resonance peak corresponds approximately to $\varepsilon_*=-1.5$, which is the condition of the second-order surface mode for a homogeneous sphere. For the doubly coated sphere, two resonance peaks have been shifted downwards.

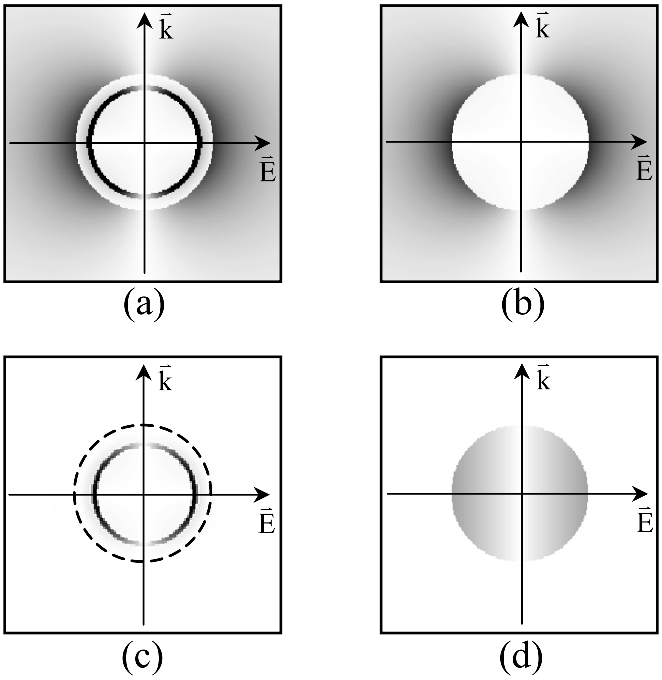

FIG. 5. Contour plots of the distribution of radial component of the scattered electric field in the E plane for a doubly coated sphere (left) and its effective sphere (right) [$\varepsilon_1=-5$, $\varepsilon_2=3$, $\varepsilon_3=10$, $\mu_1=\mu_2=\mu_3=1$, $r_1=\lambda_0/100$, $r_2=1.1r_1$, and (a,b) $r_3=1.2r_2$; (c,d) $r_3=1.31r_2$].

Figure 5 shows the contour plots of the distribution of the radial component of the scattered electric field in the E plane, to further explain how a multilayered sphere can be effectively represented by a homogeneous one in the long-wavelength limit. The parameters of the doubly coated sphere are the same as those used in Fig. 4 and the core radius is taken to be $r_1=\lambda_0/100$. When $r_3=1.2r_2$ is chosen, there are strong scattered fields in the outside region of the doubly coated sphere, as shown in Fig. 5(a). We can find that the same scattered radiation can also be produced by a single homogeneous sphere with the permittivity $\varepsilon=-0.73$ [Fig. 5(b)]. When the particle size is increased to $r_3=1.31r_2$, the two coatings can significantly cancel the scattered radiation of the core [Fig. 5(c)]. The effective permittivity of the assemblage is now close to that of the surrounding air, i.e., unity.

Compared with a coated sphere, a doubly coated sphere has introduced more free parameters to achieve the "invisibility." For a larger particle, these additional parameters can be tuned to make simultaneously zero the higher-order scattering coefficients a_n and b_n in Mie theory, realizing "invisible" bodies in the full-wave scattering case, while in the small-particle approximation, they can also provide more opportunities to achieve the transparency. For example, when a sphere with $\varepsilon_1=-2$, $\mu_1=1$, and $r_1=\lambda_0/10$ is covered with a dielectric coating with $\varepsilon_2=10$, $\mu_2=1$, and $r_2=1.1r_1$, we can employ another dielectric ($\mu_3=1$) cover to make the body "invisible." Figure 6 shows the total scattering cross section of this doubly coated sphere for different permittivity ε_3 and the cover radius r_3. We can find that there are many possibilities of ε_3 and r_3, which can be used to make the particle "invisible."

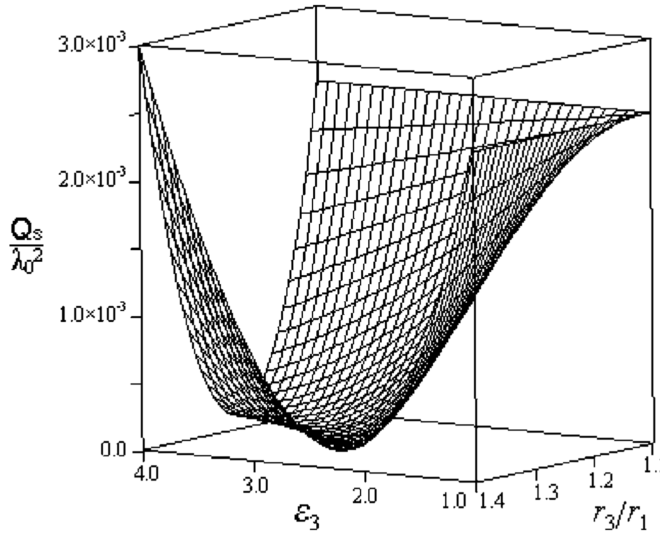

FIG. 6. Normalized total scattering cross section of a doubly coated sphere vs the permittivity ε_3 and ratio r_3/r_1 ($\varepsilon_1=-2$, $\varepsilon_2=10$, $\mu_1=\mu_2=1$, $r_1=\lambda_0/10$, and $r_2=1.1r_1$).

B. Coated spheroid

In this section, we will show how a coated spheroid can be made less observable for the EM wave. For an anisotropic core with $\tilde{\varepsilon}_1=(-3,-3,-3\eta)$ and $\tilde{\mu}_1=(1,1,1)$ covered with an isotropic coating with $\varepsilon_2=10$ and $\mu_2=1$, the values of ρ and η for which the condition (8) is satisfied for different ratio a_2/a_1 are plotted in Fig. 7. It is expected that the scattering cross section of these designed composite spheroids will be dramatically reduced in the small-particle approximation. Now we examine the ratio $a_2/a_1=1.25$. From Fig. 7, $\rho=2$ and $\eta=1.78$ are thus obtained. The full-wave analysis for such a designed composite spheroid using the commercial FEM software [19] is performed. Figure 8 shows the simulated normalized total scattering cross section for $a_1=\lambda_0/20$ in three different incident cases. As we can see, for all three cases very low total scattering cross sections are

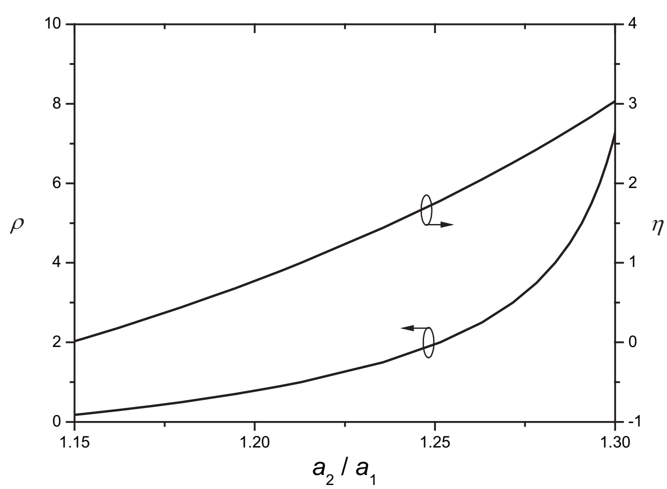

FIG. 7. Aspect ratio ρ and η for which the condition (10) is satisfied as a function of ratio a_2/a_1 for a coated spheroid [$\tilde{\varepsilon}_1=(-3,-3,-3\eta)$, $\tilde{\mu}_1=(1,1,1)$, $\varepsilon_2=10$, and $\mu_2=1$].

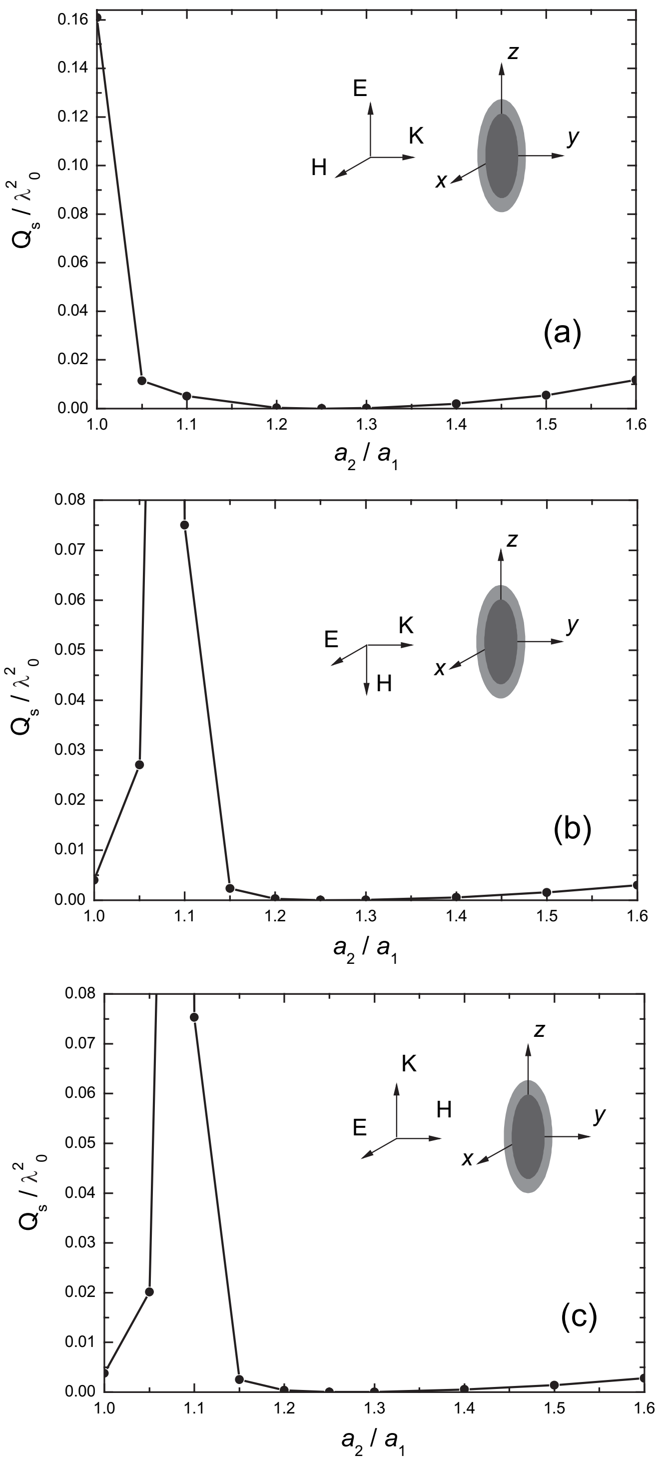

FIG. 8. Normalized total scattering cross section of a coated spheroid vs the ratio a_2/a_1 for three incident cases [$\tilde{\varepsilon}_1=(-3,-3,-5.34)$, $\varepsilon_2=10$, $\tilde{\mu}_1=(1,1,1)$, $\mu_2=1$, $\rho=2$, and $a_1=\lambda_0/20$].

observed at about $a_2/a_1=1.25$, consistent with that predicted by the quasistatic condition (8). From Figs. 8(b) and 8(c), it is found that there is a resonance around $a_2/a_1=1.1$ when the incident wave is polarized in the x-y plane. We further find that the scattering cross section is insensitive to the incident direction, and only depends on the polarization of the electric field. So we choose a coated sphere and let it have the same

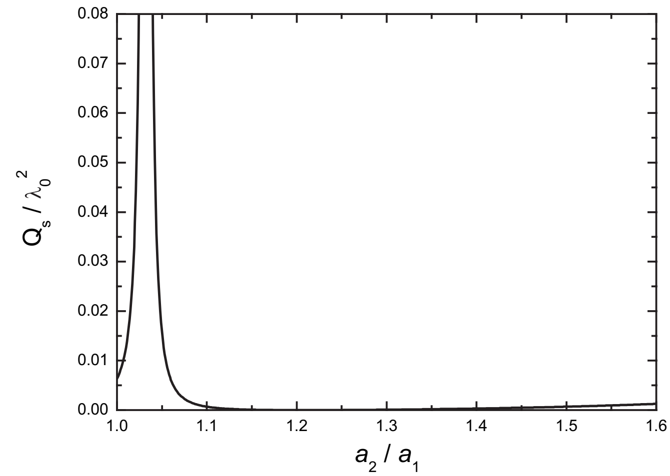

FIG. 9. Normalized total scattering cross section of a coated sphere as a function of ratio a_2/a_1 for a fixed inner core ($\varepsilon_1=-3$, $\varepsilon_2=10$, $\mu_1=\mu_2=1$, and $a_1=\lambda_0/20$).

cross section as that of the spheroid in the x-y plane to examine if the resonance still exists. In the coated sphere, the core material is isotropic and has the parameters $\varepsilon_1=-3$, $\mu_1=1$, and $a_1=\lambda_0/20$. Material parameters of the mantle in the coated sphere are the same as that in the spheroidal configuration. Figure 9 shows the normalized total scattering cross section of this coated sphere as a function of a_2/a_1. It is found that there is a resonance peak at $a_2/a_1=1.03$, deviating a little from that appearing in the coated spheroid. This similarity may imply that the resonance effect in the coated spheroid is probably due to the surface mode of the spheroidal particle.

C. Particulate composite

From the examples presented above, we have shown that electromagnetically transparent materials (multilayered sphere and coated spheroid) can be designed by using the concept of "neutral inclusion." As a final example, we will verify whether a particulate composite can be made "invisible." In the simulation, we construct a model [Fig. 10(a)] for a particulate composite mentioned in Sec. II C. In Fig. 10(a), seven spherical particles with $\varepsilon_1=-2$ and $\mu_1=1$ are embedded in a host matrix of a spherical shape with $\varepsilon_2=2$ and $\mu_2=1$. The radius of the matrix sphere is taken to be $\lambda_0/10$. For the particle arrangement, one sphere is fixed in the center of the matrix sphere; the others are all located on the axes and $\lambda_0/15$ away from the center. The radius of the particle can vary, giving different volume fractions of the particle. The full-wave simulation of this composite is conducted with commercial FEM software [19].

Figure 10(b) shows the simulated total scattering cross section (black dot) of this composite as a function of particle volume fraction c_1. Using Eq. (3), the result for its effective homogeneous sphere with the permittivity estimated from Eq. (9) is also plotted as the dashed line in Fig. 10(b). The finite-element simulation clearly shows that this composite has a very low scattering cross section at about $c_1=8.9\%$. This value is close to the theoretical prediction using the MG

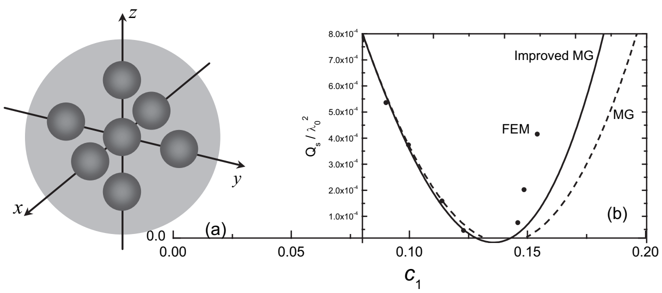

FIG. 10. (a) Sketch of a particulate composite, with material parameters $\varepsilon_1=-2$ and $\mu_1=1$ for the particle, $\varepsilon_2=2$ and $\mu_2=1$ for the matrix, and the radius of the composite sphere $\lambda_0/10$; (b) the full-wave normalized total scattering cross section of the composite (black dot) and its effective homogeneous sphere with the permittivity estimated from Eq. (9) (the dashed line) and from Eq. (10) (the solid line), vs the particle volume fraction c_1.

formula, which gives $c_1=10\%$. At the volume fraction larger than 10%, the MG-based estimation has a large deviation from the numerical simulation. One of the reasons is that the MG method does not take into account the particle interaction. Consequently, this method will underestimate the effective permittivity when the particle volume fraction increases. If the particle interaction is considered, an improved MG method [20] can be used, which is still valid for relatively high volume fraction. From this method, the effective permittivity of a particulate composite is calculated simply by [20]

$$\varepsilon_* = \varepsilon_2\left[1+\frac{3c_1(1+\Gamma^*)}{1-c_1+3\tilde{\varepsilon}(1+c_1\Gamma^*)}\right], \tag{10}$$

where $\tilde{\varepsilon}=\varepsilon_2/(\varepsilon_1-\varepsilon_2)$ and $\Gamma^*=c_1/[4(1+3\tilde{\varepsilon})^2]$. The total scattering cross section of the effective homogeneous sphere with the permittivity ε_* estimated from Eq. (10) is shown as the solid line in Fig. 10(b). It is found that a significant improvement is observed for the volume fraction larger than 10%. The remaining discrepancy may come from the fact that the multiple scattering of particles becomes important when the particle size is increased, thus the quasistatic analysis is no longer valid.

IV. SUMMARY

By introducing the concept of "neutral inclusion," we have generalized the condition for electromagnetic wave transparency found by Alù and Engheta [12]. The analytic transparency conditions for a multilayered sphere, coated spheroid, and particulate composite are derived in the quasistatic case. It is checked by the full-wave simulation that the obtained quasistatic conditions give a good prediction in the case of a small particle. For a large particle, the significant reduction of the total scattering cross section still exists, but there is a deviation from the prediction based on the quasistatic analysis. The resonance phenomenon appearing in the multilayered sphere and coated spheroid has also been discussed. All these analyses are helpful for the design of electromagnetically transparent materials.

ACKNOWLEDGMENTS

This work is supported by the National Natural Science Foundation of China under Grant No. 10325210, and the National Basic Research Program of China through Grant No. 2006CB601204.

APPENDIX

For the calculation of scattering coefficients a_n and b_n of a multilayered sphere, a recursive algorithm has been developed by Wu and Wang [21] in the framework of Mie theory. Here we use its modified version [22], and calculate the scattering coefficients from $a_n=A_n^{(L+1)}$ and $b_n=B_n^{(L+1)}$, with the help of

$$A_n^{(l+1)} = R_n(m_{l+1}x_l)\frac{m_{l+1}\mu_l H_n^a(m_l x_l) - m_l D_n^{(1)}(m_{l+1}x_l)}{m_{l+1}\mu_l H_n^a(m_l x_l) - m_l D_n^{(3)}(m_{l+1}x_l)}, \tag{A1}$$

$$B_n^{(l+1)} = R_n(m_{l+1}x_l)\frac{m_l H_n^b(m_l x_l) - m_{l+1}\mu_l D_n^{(1)}(m_{l+1}x_l)}{m_l H_n^b(m_l x_l) - m_{l+1}\mu_l D_n^{(3)}(m_{l+1}x_l)}, \tag{A2}$$

with

$$H_n^a(m_l x_l) = \frac{R_n(m_l x_l)D_n^{(1)}(m_l x_l) - A_n^{(l)}D_n^{(3)}(m_l x_l)}{\mu_{l+1}R_n(m_l x_l) - \mu_{l+1}A_n^{(l)}},$$

$$H_n^b(m_l x_l) = \frac{\mu_{l+1}R_n(m_l x_l)D_n^{(1)}(m_l x_l) - \mu_{l+1}B_n^{(l)}D_n^{(3)}(m_l x_l)}{R_n(m_l x_l) - B_n^{(l)}},$$

where

$$H_n^a(m_1x_1) = D_n^{(1)}(m_1x_1)/\mu_{l+1},$$

$$H_n^b(m_1x_1) = \mu_{l+1}D_n^{(1)}(m_1x_1),$$

$$D_n^{(1)}(z) = \psi_n'(z)/\psi_n(z),$$

$$D_n^{(3)}(z) = \zeta_n'(z)/\zeta_n(z),$$

$$R_n(z) = \psi_n(z)/\zeta_n(z),$$

$$\psi_n(z) = zj_n(z),$$

and

$$\zeta_n(z) = zh_n^{(1)}(z)$$

are Riccati-Bessel functions. According to Eqs. (A1) and (A2), a_n and b_n can be obtained by considering the initial values $A_n^{(1)}=B_n^{(1)}=0$.

[1] R. L. Fante, and M. T. McCormack, IEEE Trans. Antennas Propag. **30**, 1443 (1968).
[2] K. J. Vinoy, and R. M. Jha, *Radar Absorbing Materials: From Theory to Design and Characterization* (Kluwer Academic Publishers, Norwell, MA, 1996).
[3] J. Ward, Vacuum **22**, 369 (1972).
[4] V. G. Veselago, Usp. Fiz. Nauk **92**, 517 (1968) [Sov. Phys. Usp. **10**, 509 (1968)].
[5] J. B. Pendry, A. J. Holden, W. J. Stewart, and I. Youngs, Phys. Rev. Lett. **76**, 4773 (1996); J. Phys.: Condens. Matter **10**, 4785 (1998).
[6] J. B. Pendry, A. J. Holden, D. J. Robbins, and W. J. Stewart, IEEE Trans. Microwave Theory Tech. **47**, 2057 (1999).
[7] R. A. Shelby, D. R. Smith, and S. Schultz, Science **292**, 77 (2001).
[8] C. G. Parazzoli, R. B. Greegor, K. Li, B. E. C. Koltenbah, and M. Tanielian, Phys. Rev. Lett. **90**, 107401 (2003); A. A. Houck, J. B. Brock, and I. L. Chuang, *ibid.* **90**, 137401 (2003).
[9] Z. M. Zhang, and C. J. Fu, Appl. Phys. Lett. **80**, 1097 (2002).
[10] A. Alù and N. Engheta, IEEE Trans. Antennas Propag. **51**, 2558 (2003).
[11] J. W. Lee, M. A. Seo, J. Y. Sohn, Y. H. Ahn, D. S. Kim, S. C. Jeoung, Ch. Lienau, and Q-Han Park, Opt. Express **13**, 10681 (2005); J. W. Lee, M. A. Seo, J. Y. Sohn, D. J. Park, Y. H. Ahn, D. S. Kim, S. C. Jeoung, and Q-Han Park, J. Korean Phys. Soc. **48**, 103 (2006).
[12] A. Alù and N. Engheta, Phys. Rev. E **72**, 016623 (2005).
[13] G. W. Milton, *The Theory of Composites* (Cambridge University Press, Cambridge, 2002), pp. 113–142.
[14] G. J. C. Maxwell, Trans. R. Soc. London **203**, 385 (1904); **205**, 237 (1906).
[15] Z. Hashin and S. Shtrikman, J. Mech. Phys. Solids **11**, 127 (1963).
[16] S. Torquato, *Random Heterogeneous Materials Microstructure and Macroscopic Properties* (Springer-Verlag, New York, 2002), p. 442.
[17] C. F. Bohren and D. R. Huffman, *Absorption and Scattering of Light by Small Particles* (Wiley, New York, 1983).
[18] A. Alù and N. Engheta, J. Appl. Phys. **97**, 094310 (2005).
[19] Ansoft HFSS (High Frequency Structure Simulator), http://www.ansoft.com.cn.
[20] X. M. Zhou and G. K. Hu, Appl. Math. Mech. (to be published).
[21] Z. S. Wu and Y. P. Wang, Radio Sci. **26**, 1393 (1991).
[22] W. Yang, Appl. Opt. **42**, 1710 (2003).